UJEAS

UNIZIK JOURNAL OF ENGINEERING AND APPLIED SCIENCES

UNIZIK Journal of Engineering and Applied Sciences 3(4), September (2024), 1180 - 1196
Journal homepage: https://journals.unizik.edu.ng/index.php/ujeas
PRINT ISSN: 2992-4383 || ONLINE ISSN: 2992-4391

Coagulation performance of tiger nut chaff coagulant for treatment of fish pond wastewater: RSM and ANN machine learning Optimization

Adimachukwu M.A, Onukwuli O.D, Okey-Onyesolu C.F, Ejimofor M.I, Ohale P.E
Chemical Engineering Department, Nnamdi Azikiwe University, Awka
Corresponding Author's E-mail: mi.ejimofor@unizik.edu.ng,cf.okey-onyesolu@unizik.edu.ng, pe.ohale@unizik.edu.ng

Abstract
Chemical coagulants for wastewater treatment are sometimes expensive and environmentally hazardous, necessitating the search for eco-friendly alternatives. This study investigates the potential of Tiger nut chaff coagulant (TNCC) as a natural coagulant to treat fish pond wastewater FPW. The study focuses on optimizing the coagulation process with Response Surface Methodology and Artificial Neural Network (ANN) machine learning predictive analysis. The tiger nut chaff coagulant was extracted using a mixed salt solution procedure, and its coagulation efficiency was determined using the standard jar-testing method. The crude protein test conducted shows that TNCC contains 63.77% crude protein. The fish pond wastewater had an initial turbidity of 1213.9mg/L. After treatment, 91%, removal of the initial samples' turbidity was observed. The maximum turbidity removal efficiency was a function of the temperature, coagulant dosage, pH levels, and concentration. Optimal turbidity removal was obtained at a pH of 6, 35 o C, 3 g of coagulant, and a concentration of 175 mg/L. The RSM- ANOVA lack of fit f-value of 0.2962 at the confidence level of 95% showed an insignificant lack of fit relative to pure error. The estimated R 2 and adjusted R 2 of the ANN model were 0.93023 and 0.91907, respectively showing high capability in capturing the nonlinear nature of the coagulation treatment of the Fish Pond effluent. The statistical R values (R > 0.94) obtained from RSM and ANN modeling of the coagulation treatment indicate their significant applicability in predicting experimental values. The average relative error within the model predictions and the actual outcomes was calculated using AARE. RSM produced a lower AARE deviation parameter of 0.02074 than ANN with AARE of 0.03583 which demonstrates higher prediction accuracy and superiority of RSM over ANN. The overall result suggests that TCN is effective as an alternative to chemical coagulants, furthermore, RSM provides a more robust optimal predictive function than ANN.

Keywords: Coagulation, Tiger nut, Machine Learning, ANN, Optimization

1. Introduction

In recent years, the escalating demand for fish products has led to the expansion of aquaculture practices worldwide. However, the rapid growth of this industry has resulted in significant environmental challenges, particularly concerning the management of wastewater generated from fish farming activities (Alvanou *et al*.,2023), Fish pond wastewater typically contains high levels of organic matter, suspended solids, nutrients, and other pollutants, posing a threat to aquatic ecosystems if not adequately treated before discharge (Tabrett *et al*.,2024). Traditional wastewater treatment methods often involve the use of chemical coagulants, which can be costly and may introduce harmful chemicals into the environment (Menkiti *et al*.,2016). Therefore, there is a growing interest in exploring alternative, eco-friendly coagulants derived from natural sources (Ejimofor *et al*.,2022). Tiger nut extract, has emerged as a promising candidate due to its abundance, low cost, and reported coagulation properties.

This article aims to investigate the coagulation performance of tiger nut chaff coagulant (TNCC) extract for the treatment of fish pond wastewater. By harnessing the natural coagulant properties of TNCC, this study seeks to explore its effectiveness in removing contaminants from fish pond wastewater, thereby mitigating the environmental impact of aquaculture activities. Furthermore, the research introduces the application of Response surface methodology and artificial neural network machine learning technique for optimal prediction of the coagulation process. The integration of tiger nut coagulant as a natural coagulant, RSM, and ANN machine learning optimal prediction represents an innovative approach to addressing the challenges associated with fish pond wastewater treatment. Through rigorous experimentation and analysis, this research endeavors to contribute valuable insights into the development of sustainable and cost-effective wastewater treatment solutions for the aquaculture industry.

2.0 Material and methods
2.0 Materials and Methods

2.1. Materials

The major materials used for this work are Tiger nut residue chito-protein (CBC), and Fish pond Wastewater (FPW).

2.1.1 Material Collection
Fish pond wastewater was collected at a fish farm in Nnewi, Anambra State. Tiger nut chaff was sourced from Awka, Anambra Sate. The reagents were procured from Bridge-head market, Onitsha.

2.1.2 Material Characterization
The wastewater was characterized before and after the treatment at the Department of Chemical Engineering Laboratory, Nnamdi Azikiwe University, Awka, Anambra state. Parameters of interest such as effluent turbidity, pH, total solids (TS), total suspended solids (TSS), total dissolved solids (TDS), total hardness, chemical oxygen demand (COD), dissolved oxygen (DO), biochemical oxygen demand (BOD), heavy metals, conductivity, and colour. The parameters and the respective standard testing methods used are presented in Table 1. Furthermore, after coagulant extraction, the extracted coagulant was characterized using the test methods in Table 2.

Table 1: Physico-chemical testing methods for wastewater

Parameters	Standard methods
Temperature	AWWA, 1985; Nieswiadomy, 1992
PH	APHA, AWWA, 423 - 1985; Clark, 1999
Total suspended solid (TSS)	APHA, AWWA, 209C – 1985, Van Staden & Haarhoff, 2011.
Total dissolved solid (TDS)	APHA, AWWA, 209B – 1985
Total solid (TS)	APHA, AWWA, 205 – 1985
Turbidity	APHA, AWWA, 214 - 1985; Baalsurd *et al*, 1994
Chemical Oxygen Demand (COD)	ASTM D1252-06 (2012)
Biochemical Oxygen Demand (BOD)	ASTM 5210B (1999)

AWWA: American water works association, APHA: American public health association

2.1.3. Extraction of coagulant from Tiger nut chaff coagulant
Coagulant extraction from Tiger nut chaff was done using a mixed salt solution method (Okey-Onyesolu *et al*., 2020). Exactly 1000g of raw tiger nut chaff was sun-dried, and ground using an industrial grinder. The grounded samples were sieved using a 0.6 mm sieve. A mixture of salt solution consisting of 0.7 g/l of calcium chloride, 4 g/l of magnesium chloride, 0.75 g/l potassium chloride, and 30g/l sodium chloride was mixed in a 1000 ml beaker. The ground tiger nut chaff was poured into the 1000 ml beakers containing salt solution in the ratio of 1:10 (w/v) (solid-solution ratio). The mixture was stirred for 2 hours using a magnetic stirrer at a temperature of 70 ^{0}c. The resulting suspension was filtered using muslin cloth. The filtrate was allowed for 30 minutes to settle before decanting to concentrate the bio-coagulant. The concentrated bio coagulant was dried and crushed to obtain the coagulant in

powdered form.

Table 2. Characterization procedure for bio-coagulants

Parameters	**Procedure**
Moisture content (% dry weight)	AOAC 934 (2005), Feldsine *et al.*,2015
Crude protein (%)	AOAC- 920.53 (2012). Bonysana *et al*.,2024
Ash content (%)	AOAC -942.05 PA(2000), Bonysana *et al*,2024
Crude fibre content (%)	
Lipid content (%)	AOAC – 999.02(1999), Ejimofor *et al*.,2020
Carbohydrate by diff (%)	Ejimofor *et al*.,2020

AOAC: Association of analytical chemistry, ASTM: American standard of testing material

2.1.4 Jar test

Coagulation experiments were conducted in 1000ml cylindrical beakers (10 cm diameter) using conventional jar-test apparatus. The Tiger nut chaff coagulant (TNCC) was dosed into the 500 ml of the wastewater samples. The TNCC dosages were varied from 1 g/l – 5 g/l. The resulting mixtures of TNCC and wastewater samples were stirred rapidly at 200 r/min for 2 minutes, followed by slow mixing of 30 r/min for 20 minutes. After that, the treated effluents was allowed to settle for 50 minutes. During the settling time, 20 ml of supernatant samples were withdrawn by syringe from about 2 cm depth below the water surface into 50 ml turbidity measuring container (Menkiti *et al.*, 2016). Turbidity was measured and recorded immediately after the stirring seized; the measuring and recording were continued at an interval of 5 minutes during the 50 minutes settling time (zemagu *et al*., 2021)

Plate 1: Fishpond effluent coagulation procedure (fish pond effluent stirring on magnetic stirrer)

2.1.5 Design of Experiment Using Response Surface Methodology

Table 3. CCD summary for fish pond effluent coagulation.

Independent variables		Coded variable levels				
		-α	-1	0	+1	+α
Temperature	minute	27.5	30	35	40	42.5
Dosage	C	1.5	2	3	4	4.5
pH	-	3	4	6	8	9
Concentration	-	175	300	550	800	925

Stat-ease, incorporation design expert software 10.0 central composite Design (CCD) design was chosen to analyze the samples. CCD provides high-quality predictions over the entire design space because it generates new extremes for all factors outside the design bracket (Ejimofor *et al*.,2021; Okey-Onyesolu *et al*.,2020). The high and low values were selected while the software generated the alpha high and alpha low values. These points are called the star points of the design. The summary of the 3-level factor design used in this work is shown in Table 3 for fish pond coagulation, while Table 4 shows the design matrix for the coagulation experiment.

Table 4: CCD table for PW in terms of actual process factors

	Factor 1	Factor 2	Factor 3	Factor 4
Run	A: Temp.	B: Dosage	C: Ph	D: Conc.
	Deg. C	g/L		mg/L
14	30	2	4	300
11	40	2	4	300
25	30	4	4	300
24	40	4	4	300
26	30	2	8	300
7	40	2	8	300
15	30	4	8	300
20	40	4	8	300
5	30	2	4	800
13	40	2	4	800
12	30	4	4	800
18	40	4	4	800
17	30	2	8	800
29	40	2	8	800
23	30	4	8	800
8	40	4	8	800
19	27.5	3	6	550
30	42.5	3	6	550
1	35	1.5	6	550
2	35	4.5	6	550
22	35	3	3	550
9	35	3	9	550
3	35	3	6	175
16	35	3	6	925
10	35	3	6	550
4	35	3	6	550
6	35	3	6	550
21	35	3	6	550
27	35	3	6	550
28	35	3	6	550

2.1.6 Artificial Neural Network (ANN)

ANN is designed and well suited for pattern recognition (Ejimofor *et al.77*.,2020); the experimental data was sequentially inserted with the input variables and the corresponding responses as obtained to the experimental run array of the RSM. The number of neurons required in the hidden layer was determined by trial and error method to minimize the deviation of predictions from experimental results. At the end of several trials, 6 hidden neurons were required to build the final model. The ANN architecture used for this study is shown in Fig 3.6. The input layers have four (4) neurons with each neuron representing the respective input variables (pH, settling time, dosage, and temperature) and four target neurons with each target neuron representing the response variables (Turbidity).

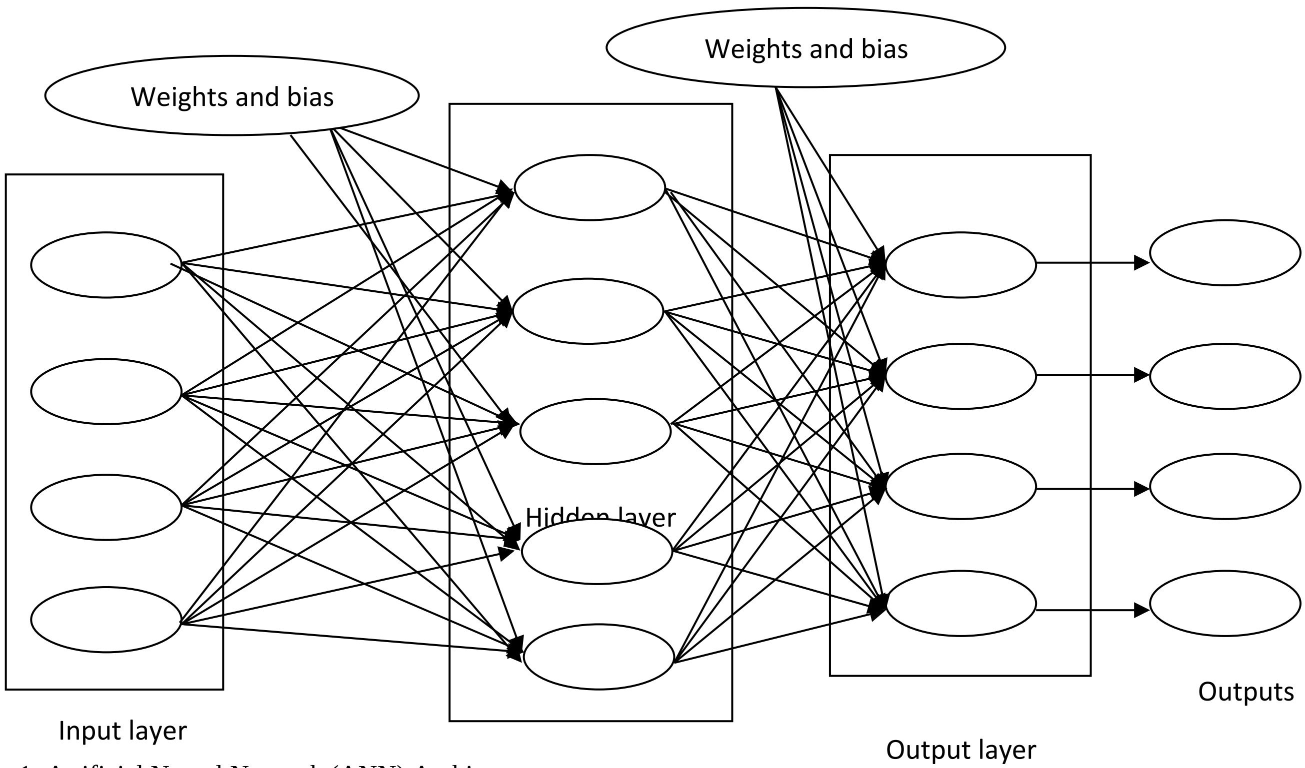

Fig 1: Artificial Neural Network (ANN) Architecture.

The architecture in Fig 1 shows that there were five (5) hidden neurons in the hidden layer. Each of the hidden neurons has the log-sigmoid model embedded in it. The log-sigmoid model is seen in Equation 1.

$$logsig(n) = \frac{1}{1+e^{-n}} \quad (1)$$

Where n is the input variable data.

3.0 Results and Discussions

3.1 **Wastewater characterization**

To ascertain the initial condition of the fishpond wastewater, the samples were characterized comprehensively using standard methods of wastewater analysis (*AWWA: American Water Works Association, APHA: American Public Health Association)* and compared with the recommended discharge limits from environmental agencies (WHO, FEPA, and NESREA). The results of selected physicochemical parameters from the characterization of the fishpond wastewater samples are presented in Table 5. It is obvious from Table 5 that the pollution indicators were significantly substantial, highlighting the need for treatment before discharge. The turbidity, which gives a measure of the relative clarity of the effluents, was above 500% higher than the discharge limits. This high level of turbidity could be attributed to the peculiar nature of the effluent. According to Menkiti *et al*., (2021), the high turbidity of fishpond effluent is attributed to wastes accumulated through feeding activities, unconsumed food particles, activities of microorganisms, and excreta of the fishes inside the ponds which also affect the COD and TSS levels. It is important to note that turbidity affects every other aspect of water quality (Okolo *et al*., 2021).

The amount of dissolved oxygen required by aerobic microorganisms to act on organic substrates (BOD) was also observed to be higher than the discharge limits lightly higher in fishpond than the paint effluent. The COD/BOD_5 ratio was used to ascertain the most suitable treatment approach for effluent. The biodegradable fraction is dominant if the COD/BOD_5 ratio is less than 3.0, while the inert portion is significant if the same parameter is above 3.5 (Hurskainen, 2020). It is important to highlight that a biological treatment approach is recommended when the COD/BOD_5 is below 3.0. From the obtained results, COD/BOD_5 ratio was within the range of $3.04 \leq COD/BOD_5 \leq 3.41$, suggesting that biological treatment will not be feasible to eliminate the target pollutants. Furthermore, given that the COD/BOD_5 parameter was within 3.0 and 3.5, it follows that a physicochemical process such as coag-flocculation will be the most appropriate remediation procedure for fishpond effluent. Despite these harmful pollution indices, it is noteworthy to state that the effluent pH of the sample was within the discharge limits stipulated by the environmental agencies.

Table 5: wastewater characterization parameters

Parameter		Discharge limits		
	Raw effluent	NESREA	FEPA	WHO
pH	7.8±0.6	6 – 9	6 – 9	6.8– 8.2
Turbidity (NTU)	581	-	< 100	< 11.75
Turbidity (mg/L)	1213.928	-	-	-
Biochemical oxygen demand (BOD_5), mg/L	358 ± 1.09	30	210	40
Chemical oxygen demand, mg/L	1088.32 ± 11.6	60	< 180	250
COD/BOD_5	3.04 ± 0.19	-	-	-
Total organic carbon, mg/L	80 ± 0.18	-	-	-
Total phosphorus, mg/L	-	3.5	-	5.0
Total suspended solids, mg/L	998.14 ± 1.61	25	< 100	< 50
Total solids, mg/L	-	1000	< 2000	500
Total dissolved solids, mg/L	-	500	-	< 500
Ammonia Nitrogen, mg/L	98 ± 0.13	15	-	10
Nitrate, mg/L	9.97 ± 0.26	-	-	-
Potassium, mg/L	23.1 ± 0.02	-	-	-
Colour, Pt scale (mg/L)	Green solid	-	-	-
Odor	Objectionable	Odorless	Odorless	Odorless

3.2 Characterization of the extracted coagulant

To understand the physical, chemical, and structural pattern of the coagulant, both proximate (conducted on the coagulant precursor) and selected instrumental analyses (on the extracted bio-coagulant) were conducted.

3.2.1 Proximate analysis

The proximate analysis results for bio-coagulant precursor (tiger nut chaff) are presented in Table 6. The results confirmed the presence of protein content, crude fibre, carbohydrate, lipid content, and ash in the tiger nut chaff. Table 6 revealed that the highest constituent of the sample is the crude protein. The high crude protein content is a strong point in favour of its usage as a bio-coagulant. This point is consistent with literature reports; as the high protein presence is indicative of good coagulation characteristics. The ash content is an indication of the presence of carbon compounds and inorganic components in the form of salts and oxides in the crab shell, fish bone, fish scale, and eggshell (Usman *et al.*, 2006). Carbon plays a vital role in the adsorption of substances due to its porous nature; this is an indication that precursor samples in their granular or ash form can play a vital role in the removal of metals and other particles from the solution. It can remove colour and some other precursors of gaseous substances that generate odour and smell in wastewater. The presence of fibre contents also shows that the precursor is an organic polymer with repeating small molecules that could extend as tails and loops when dispersed in water. Also, the fibre content enhanced the strength of the precursor samples (Ji et *al*., 2024); apart from its hardness and toughness, it was observed that the fibrous content of the samples contributed immensely to its ability to remove insoluble particles from the solution, hence serving as a semi-permeable medium; it can also remove some heavy particles from solution The moisture content values show the precursors' ability to absorb water easily. The findings from Table 6 (with a special interest in the crude protein and fibre contents) suggest the potency of the animal extracts as an effective coagulant.

Table 6 Results of proximate analyses of the bio-coagulants

	Parameters		TNC
1.	Moisture content (%)	18.83	
2.	Crude protein (%)		63.77
3.	Ash content (%)	3.80	
4.	Crude fibre (%)	2.35	
5.	Lipid content (%)	6.40	
6.	Carbohydrates (%)		4.85

3.2.2. Instrumental Anayses

3.2.2.1 SEM analysis

SEM assay illustrates the particle size, porosity, and other morphological features of any given sample. Plate 2 depicts the SEM micrograph of raw, activated, and spent TNCC, respectively. The surface micrograph of TNCC (see Plate 2a) portrays the existence of a layer – piled structure characterized by irregular flakes; a distinct property of highly fibrous chelation materials. The external micrograph of the activated sample (Plate 2b) reveals the development of enhanced surface cohesion and flocked porous field matrix. These attributes demonstrate that the sample activation procedure significantly improved the outer heterogeneous properties of TNCC which are necessary for surface-driven matrices (Osman *et al*.,2023; Ohale *et al*., 2021). Such surface can create highly rated sites for particles adsorption.

Plate 2c shows the surface morphology of spent TNCC. This surface elucidates a complete disappearance of the dark porous flock template observed in Plate 2b. In comparison to the raw TNCC (Plate 2a) the SEM images of the spent sample depict a flattened river – like surface. These reduced porosity and surface saturation features validate its effectiveness in the adsorptive treatment of fishpond wastewater. Hence it can be inferred that the particles in the treated fishpond wastewater were adsorbed onto the pores of the TNCC leading to reduced porosity as compared with the surface morphology of TNCC prior to the coagulation process.

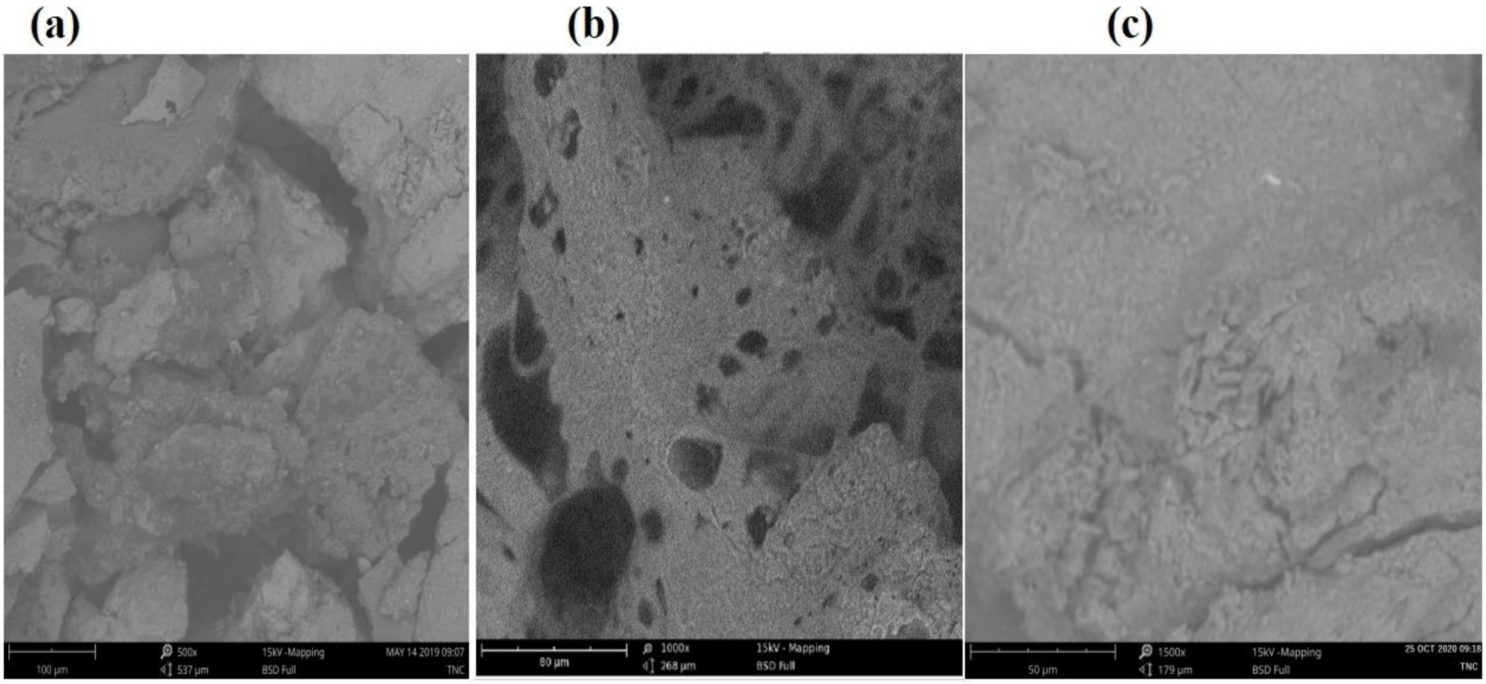

Plate 2: SEM image of (a) raw TNCC, (b) activated TNCC, and (c) spent TNCC.

3.2.2.2 **XRF**

The elemental composition of TNCC was obtained via the XRF. The results as presented in Table 7 indicate that the prominent elements (aside from Oxygen) in TNCC are sodium (33.25 %), calcium (27.06 %), Aluminium (13.69 %), and Phosphorus (18.56 %). Calcium and Carbon- rich substances have been identified as highly desirable chelation materials for surface-driven uptake of various pollutants (Menkiti *et al.*,2022). The charged surfaces provided by these compounds induce charge neutralization in the bulk of the wastewater sample during coagulation. In-turns the charged-neutralized suspended particles tend to form bridges with one another. Menkiti *et al.*, 2020 refer to this stage as inter-particle bridging stage which then progress to floc formation during the flocculation stage.

Table 7: XRF analysis of raw CBCC and TNCC coagulants

Element	**TNCC**	
	Atomic Conc.	**Weight Conc.**
Oxygen	-	-
Carbon	-	-
Sodium	33.25	25.13
Nitrogen	-	-
Aluminium	13.69	12.14

Potassium	0.67	0.86
Sulfur	1.36	1.43
Calcium	27.06	35.65
Phosphorus	18.56	18.9
Magnesium	2.35	1.88
Silicon	2.4	2.21
Iodine	0.25	1.04
Iron	0.41	0.76
Total	100	100

4.1.5 XRD

The X-ray diffraction pattern of TNCC is depicted in Fig 2. The XRD pattern of TNCC demonstrates conspicuous peaks at 2θ = angle of 10.37. 13.7, 17.6, 20.6 and 25.4^0. The characteristic peak at 25.4^0 which corresponds to the plane (004) indicates the existence of extremely organized crystalline cellulose (Obele *et al.*,2021). These well-resolved peaks are typical of C - type diffraction patterns of starch-based materials (Onuzulike *et al.*,2023)

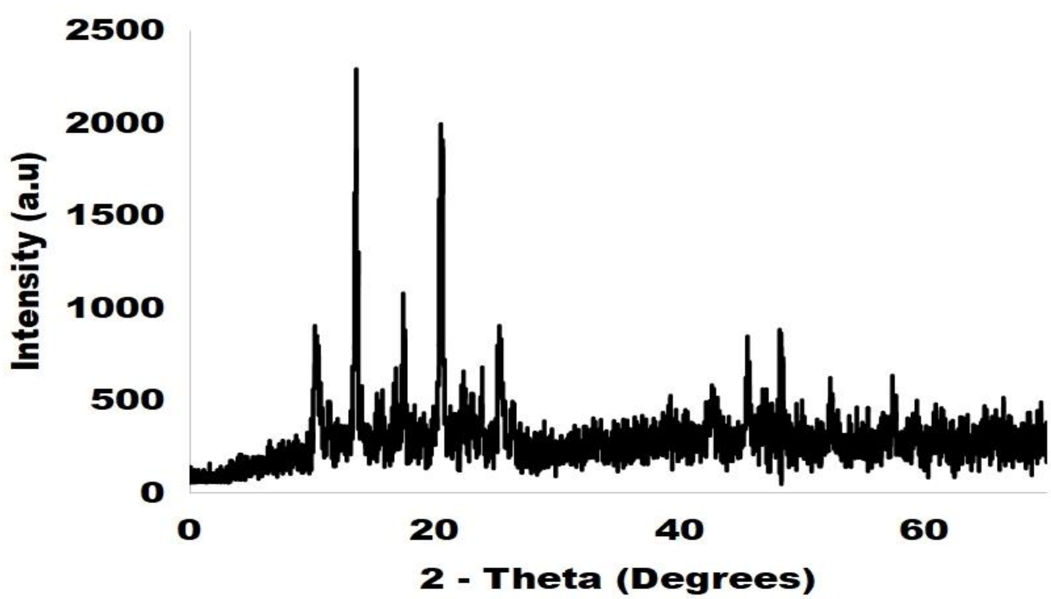

Fig. 2: XRD pattern of TNCC coagulants.

4.8.1 Fishpond effluent coagulation optimization

Results obtained from the respective experimental runs are presented in Table 8. For the coagulation system using TNCC, the Table 8 below was analyzed using the design expert to obtain the design equation and the relevant optimization parameters.

Table 8: Design of experiment result for FP-TNCC (Turbidity removal)

Std	Run	A:Temp.	B:Dosage	C:pH	D:Conc.	Turb. Rem. Eff.
		Deg. C	g/L		mg/L	%
1	14	30	2	4	300	77.76
2	11	40	2	4	300	80.43
3	25	30	4	4	300	65.58
4	24	40	4	4	300	67.46
5	26	30	2	8	300	67.31
6	7	40	2	8	300	67.98
7	15	30	4	8	300	63.72
8	20	40	4	8	300	64.88
9	5	30	2	4	800	42.59
10	13	40	2	4	800	45.93
11	12	30	4	4	800	33.05
12	18	40	4	4	800	35.74
13	17	30	2	8	800	39.09
14	29	40	2	8	800	41.41
15	23	30	4	8	800	34.48
16	8	40	4	8	800	36.15
17	19	27.5	3	6	550	52.49
18	30	42.5	3	6	550	56.68
19	1	35	1.5	6	550	71.21
20	2	35	4.5	6	550	56.8
21	22	35	3	3	550	73.99
22	9	35	3	9	550	69.59
23	3	35	3	6	175	91.35
24	16	35	3	6	925	37.3
25	10	35	3	6	550	75.08
26	4	35	3	6	550	73.86
27	6	35	3	6	550	74.53
28	21	35	3	6	550	71.5
29	27	35	3	6	550	80.5
30	28	35	3	6	550	73.41

4.8.1.1 RSM modeling and ANOVA analysis for fishpond effluent coagulation

The analysis of the result of the experimental design presented in Table 9, demonstrates the pertinent ANOVA parameters that were computed from response surface modeling.

Table 9: ANOVA values and mode test of significance for turbidity removal

	Full quadratic model					Reduced quadratic model				
source	sum of squares	Df	mean squares	F-value	p - value	sum of squares	df	mean squares	F-value	p - value
$x_1 = \text{temp}$	25.1	1	25.1	4.59	0.049	25.1	1	25.1	5.63	0.0284
$x_2 = \text{dosage}$	336.49	1	336.49	61.5	0.0001	336.49	1	336.49	75.41	0.0001
$x_3 = \text{pH}$	78.52	1	78.52	14.35	0.0018	78.52	1	78.52	17.6	0.0005
$x_4 = Conc$	5240.1	1	5240.1	957.8	0.0001	5240.1	1	5240.1	1174.32	0.0001
x_1x_2	0.16	1	0.16	0.0292	0.8665	-	-	-	-	-
x_1x_3	1.42	1	1.42	0.2588	0.6183	-	-	-	-	-
x_1x_4	0.8281	1	0.8281	0.1514	0.7027	-	-	-	-	-
x_2x_3	50.13	1	50.13	9.16	0.0085	50.13	1	50.13	11.23	0.0034
x_2x_4	0.3136	1	0.3136	0.0573	0.814	-	-	-	-	-
x_3x_4	27.98	1	27.98	5.11	0.039	27.98	1	27.98	6.27	0.0215
x_1^2	980.25	1	980.25	179.17	0.0001	980.25	1	980.25	219.67	0.0001
x_2^2	295.4	1	295.4	53.99	0.0001	295.4	1	295.4	66.2	0.0001
x_3^2	30.43	1	30.43	5.56	0.0323	30.43	1	30.43	6.82	0.0172
x_4^2	279.14	1	279.14	51.02	0.0001	279.14	1	279.14	62.55	0.0001
	ANOVA					ANOVA				
Model	8047.2	14	574.8	105.06	0.0001	8044.5	10	804.46	180.28	0.0001
Lack of fit	35.72	10	3.57	0.3854	0.9065	38.44	14	2.75	0.2962	0.9671
Residual	82.07	15	5.47			84.78	19	4.46		
Pure error	46.35	5	9.27			46.35	5	9.28		
Adequacy precision = 34.08						Adequacy precision = 43.846				
C. V. (%) = 4.04						C. V. (%) = 3.65				
Mean = 57.94						Mean = 54.94				

The p-value was used in the ANOVA approach to assess the sufficiency and quality of fit of the mathematical models. A certainty level of 95% was employed to analyze the likelihood of the p-value; as a result, the importance of the relevant model term increased with decreasing p-values (p-values 0.05), and vice versa (Ohale *et al*., 2023). Table 9 illustrates the entire quadratic models and the reduced quadratic models that were produced after the insignificant model terms were deleted. Consequently, the produced RSM models for predicting turbidity removal efficiencies from fishpond effluent were stated in Equation 2. In addition to the p-values, the f-values may be used to determine the importance of every component in the quadratic equation. This was accomplished by evaluating the ratio between the mean square and the residual error of the quadratic model. Hence, by comparing the models' lack of fit parameters for the reduced quadratic model, F-values generated for turbidity (180.28), removal implied that the quadratic models were significant relative to the pure error. The lack of fit f-value (turbidity = 0.2962) highlights an insignificant lack of fit relative to the pure error. Associated lack of fit p-value indicates that there is a very high probability (turbidity = 96.71%;) that the f-values for lack of fit are a result of noise. Furthermore, the predicted R–squared values (turbidity = 0.9805) were in acceptable accord with the adjusted R–squared (turbidity = 0.9694), consequently indicating the reproducibility of the RSM models (Onu *et al*., 2022). The predicted versus actual plots displayed in Fig 3 were further used to assess the reliability of the quadratic model. It was depicted from the figure that the experimental and predicted values visibly aligned along the diagonal lines authenticating the reliability of the model predictions.

The adequacy precision measurement (APR) provides a clue as to the signal-to-noise ratio. Rout et al., (2023), assert that a model needs an APR larger than 4.0 to successfully traverse the design space. Hence, the estimated APR values (Turbidity = 43.846) registered in this study indicate the existence of sufficient signals relative to the noise. Besides, the approximated values of the coefficient of variance (CV) (Turbidity = 3.65) satisfactorily authenticated the reproducibility of the quadratic models.

$$Turb.Rem.(\%) = 26.211x_1 + 21.211x_2 - 0.1821x_3 + 0.0074x_4 + 0.885x_2x_3 + 0.002645x_3x_4 - 0.37128x_1^2 - 5.095x_2^2 - 0.4088x_3^2 - 0.000079x_4^2 - 396.995 \quad (2)$$

The result obtained from the solving equation Equation 2, shows optimal turbidity removal efficiency of 91% at pH of 6 and 35^{o}C.

ANN modeling

The graphical expression for the topological evaluation of ANN is presented in Figs. 3. Data screening and partitioning (as a training set and test set) were executed to eliminate over-training and over-parameterization. The ANN architectural network was developed using 10 hidden neurons, 4 input neurons, and one output layer (4-10-1). Furthermore, the correlation coefficients obtained from the regression plots (training = 0.99939, validation = 0.87069, testing = 0.99408, all = 0.96803) signaled a high correlation between experimental data and ANN model predictions. The graphical illustration of the validation function given in Fig. 4 was used to measure the reliability of the training process. The best validation performance of the training networks generated a mean square error of 0.0083734. The negligible mean square error value recorded for the study demonstrated the absence of any over-fitting complication within the neural network. The estimated R^2 and adjusted R^2 of the ANN model were 0.9025 and 0.8945, respectively. Significant R^2 values established for ANN models authenticate its capability in capturing the nonlinear nature of the coagulation treatment of fishpond effluent.

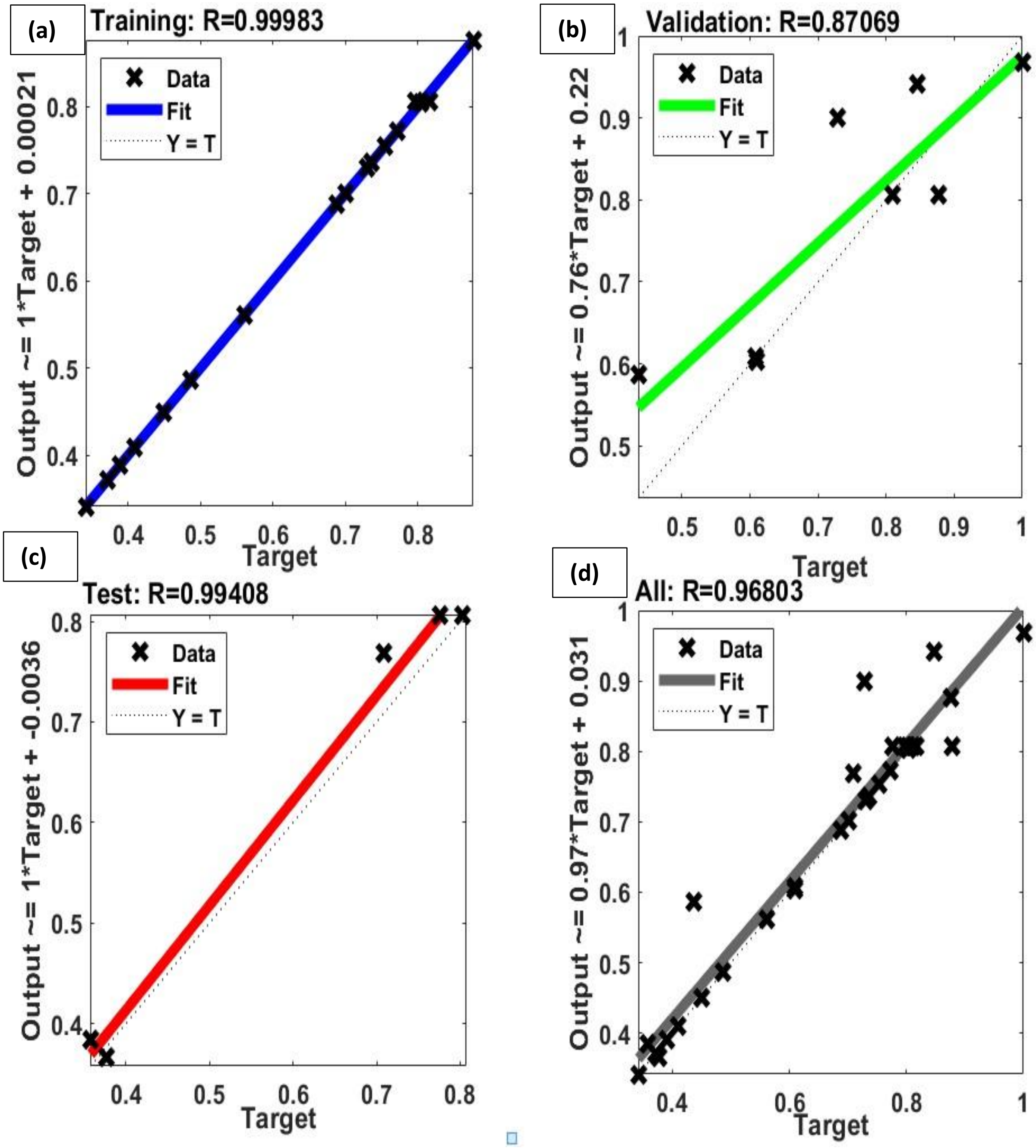

Fig. 3. ANN model turbidity removal plots for(a) training (b) validation (c) testing (d) all data.

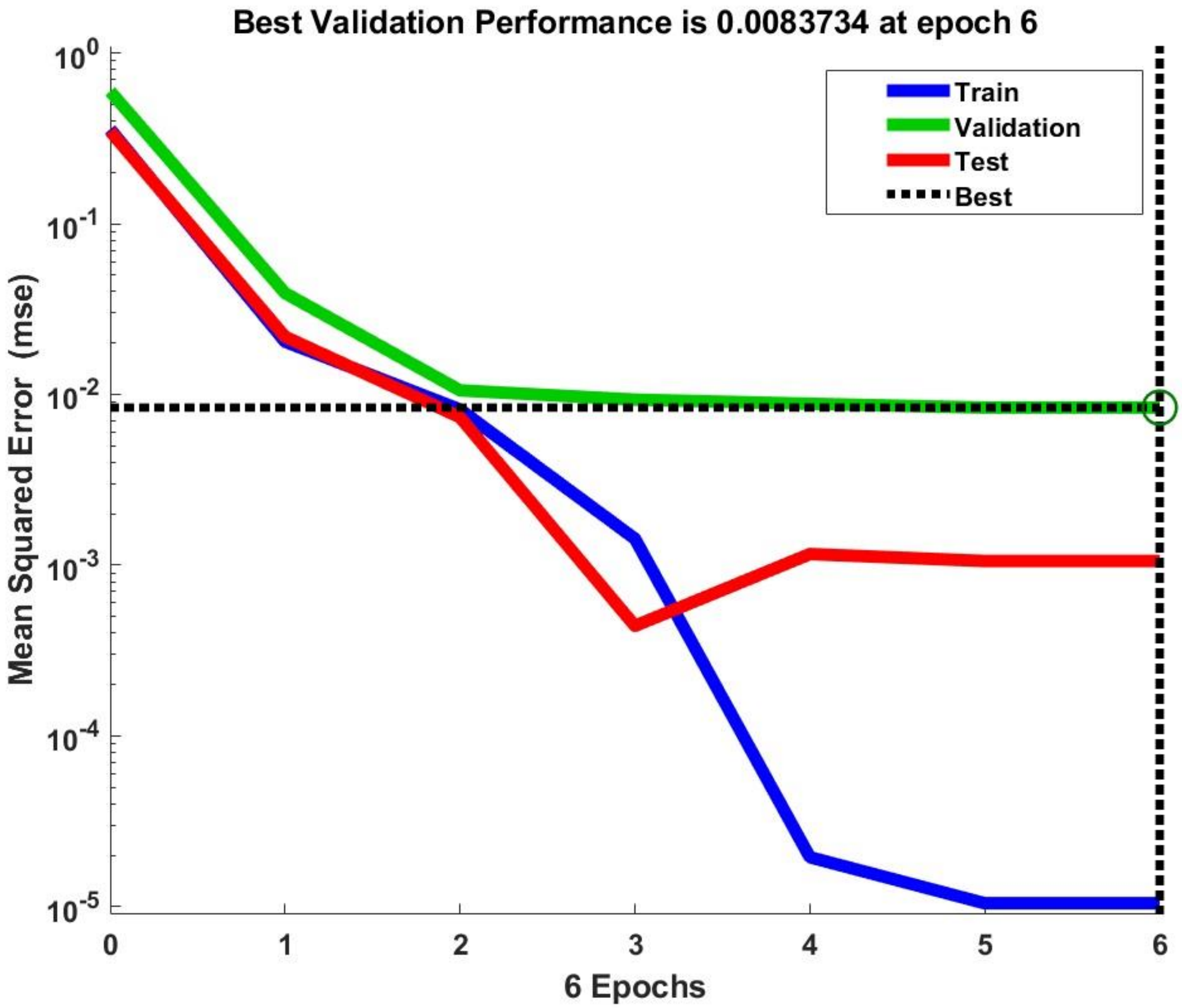

Fig. 4: ANN model turbidity validation plot

Comparison of RSM and ANN

The precision of established models (RSM, and ANN) in estimating the turbidity removal efficiency from fishpond effluents was appraised by comparing their predicted values with experimental values using error function models. The obtained results are presented in Table 10. For a satisfactory relationship between empirical and predicted results, R should be more than 0.8. Hence, the high R values (R > 0.94) obtained from RSM and ANN modelling of the coagulation treatment indicates their significant applicability in predicting experimental values. The effectiveness of both algorithms' values in predicting the rates of turbidity removal from fishpond effluent was validated by the use of adjusted R^2, which measures the level of R^2 overestimation. The average relative error within the model predictions and the actual outcomes was calculated using AARE. RSM produced a lower AARE deviation parameter than ANN which demonstrated its higher prediction accuracy and superiority over ANN. MPSE calculates a system's geometric deviation distribution and permits multiple degrees of freedom. The values of MPSE obtained for turbidity removal from fishpond effluent using RSM were 0.03066 while using ANN, 0.08984 was obtained. Low error magnitudes obtained by testing other statistical indicators (RMSE, SD, HYBRID) on the outputs (Table 10) further gave credence to the superiority of the RSM model in the data prediction accuracy of the present study. In general, results obtained from statistical analysis indicate that RSM was superior to ANN in the optimization of the coagulation treatment of fishpond effluent using TNCC (also see Fig 4). The results obtained here correlate favorably with the findings of other researchers who noted the superior prediction accuracy of RSM over ANN in process modelling (Ray *et al*., 2021; Nazerian *et al*., 2018).

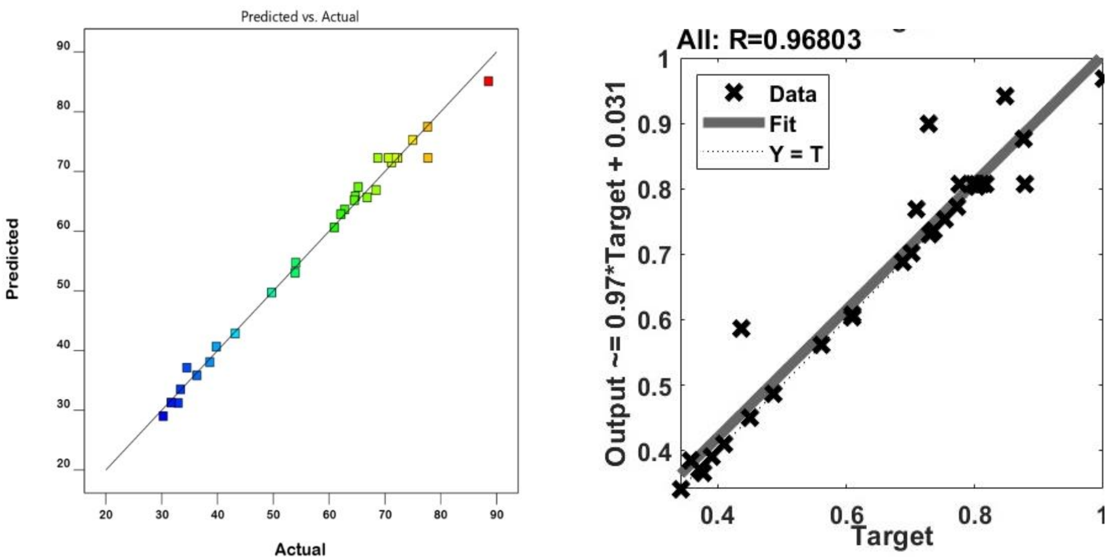

Fig 4: Predicted vs actual plot (a) for RSM (b) for ANN

Table 10: Statistical appraisal indices of RSM, and ANN for fishpond coagulation

	Turbidity	
Parameter	RSM	ANN
R	0.99020	0.97407
R^2	0.9805	0.94882
Adj-R^2	0.9694	0.94063
AARE	0.02074	0.03583
MPSE	0.03066	0.08984
RMSE	0.02855	0.08363
SEP	0.04141	0.12132
HYBRID	5.18637	40.28977

4.0 Conclusion

The coagulation performance of tiger nut chaff coagulant (TNCC) in fishpond wastewater using response surface methodology and the Adaptive Neuro-Fuzzy Inference System (ANFIS) for optimization demonstrates that TNCC extracted using salt solution method effectively decreased to dischargeable limit the pollutant of the target (colloidal particles causing turbidity) in fish pond wastewater. The experimental result from the central composite design (CCD) and response show that maximum turbidity removal is a function of the temperature, coagulant dosage, pH levels, and concentration. The comparison of the predictive analysis of the RSM and the ANFIS shows that the RSM was more robust in predicting the optimal removal conditions than the ANFIS. Conclusively, this study portrays TNCC as a sustainable, cost-effective alternative to chemical coagulants. Fish producing and process industry should leverage on this to treat and enhance their wastewater quality before discharge to the environment.

Furthermore, the use of TNCC is recommended for use as coagulant for treatment of other highly turbid wastewaters such as paint industrial wastewater and textile industries wastewater.

5.0 Recommendation

It is recommended that TNCC should be used for the treatment of other effluent via coagulation method to establish its efficiency for industrial effluents other than fishpond wastewater. Also TNCC should be adopted by fish farmers for treatment of their effluent before discharge.

References

Alvanou, M.V., Gkagkavouzis, K., Karaiskou, N., Feidantsis, K., Lattos, A., Michaelidis, B., Theodorou, J.A., Batargias, C., Triantafyllidis, A. and Giantsis, I.A., 2023. Mediterranean aquaculture and genetic pollution: A review combined with data from a fish farm evaluating the ecological risks of finfish escapes. *Journal of Marine Science and Engineering*, *11*(7), p.1405.

Bonysana, R., Singh, K. D., Devi, W. D., Koijam, A. S., Kapesa, K., Kalita, J., ... & Rajashekar, Y. 2024. Ethno-entomotherapeutic and metabolite profiling of Coridius chinensis (Dallas), a traditional edible insect species of North-East India. *Scientific Reports*, *14*(1), 6545.

Clark, R. M. 1999 Water quality modeling--case studies. *Water distribution systems handbook. New York: McGraw Hill*.

Ejimofor, M. I., Ezemagu, I. G., & Menkiti, M. C. 2020. Biogas production using coagulation sludge obtained from paint wastewater decontamination: Characterization and anaerobic digestion kinetics. *Current Research in Green and Sustainable Chemistry*, *3*, 100024.

Ejimofor, M. I., Ezemagu, I. G., & Menkiti, M. C. 2021. RSM and ANN-GA modeling of colloidal particles removal from paint wastewater via coagulation method using modified Aguleri montmorillonite clay. *Current Research in Green and Sustainable Chemistry*, *4*, 100164.

Ejimofor, M. I., Ezemagu, I. G., Ugonabo, V. I., Nnaji, P. C., Anadebe, V. C., Diyoke, C., & Menkiti, M. C. 2022. Adsorption kinetics, mechanistic, isotherm and thermodynamics study of petroleum produced water coagulation using novel Egeria radiate shell extract (ERSE). *Journal of the Indian Chemical Society*, *99*(3), 100357.

Ezemagu, I. G., Ejimofor, M. I., Menkiti, M. C., & Nwobi-Okoye, C. C. 2021. Modeling and optimization of turbidity removal from produced water using response surface methodology and artificial neural network. *South African Journal of Chemical Engineering*, *35*, 78-88.

Feldsine, P., Kaur, M., Shah, K., Immerman, A., Jucker, M., & Lienau, A. 2015. AOAC Official Method SM Matrix Extension Validation Study of Assurance GDSTM for the Detection of Salmonella in Selected Spices. *Journal of AOAC International*, *98*(4), 930-938.

Hurskainen, H. 2020. Pre-treatment requirements for challenging wastewater streams from new biochemical process to enable aerobic treatment.

Menkiti, M. C., Aniagor, C. O., Onuzulike, C. M., Ejimofor, M. I., & Okonkwo, S. S. 2022. Chromium adsorption from petroleum refinery wastewater using biocomposites. *Results in Surfaces and Interfaces*, *8*, 100064.

Menkiti, M. C., Ejimofor, M. I., Ezemagu, I. G., & Uddameri, V. 2016. Turbid-metric approach on the study of adsorptive component of paint effluent coagulation using snail shell extract. *Arabian Journal for Science and Engineering*, *41*(7), 2527-2543.

Nieswiadomy, M. L. 1992. Estimating urban residential water demand: Effects of price structure, conservation, and education. *Water Resources Research*, *28*(3), 609-615.

Obele, C. M., Ejimofor, M. I., Atuanya, C. U., & Ibenta, M. E. 2021. Cassava stem cellulose (CSC) Nanocrystal for optimal methylene BlueBio sorption with response surface design. *Current Research in Green and Sustainable Chemistry*, *4*, 100067.

Okey-Onyesolu, C. F., Chukwuma, E. C., Okoye, C. C., & Onukwuli, O. D. 2020. Response Surface Methodology optimization of chito-protein synthesized from crab shell in treatment of abattoir wastewater. *Heliyon*, *6*(10).

Okey-Onyesolu, C. F., Onukwuli, O. D., Ejimofor, M. I., & Okoye, C. C. 2020. Kinetics and mechanistic analysis of particles decontamination from abattoir wastewater (ABW) using novel Fish Bone Chito-protein (FBC). *Heliyon*, *6*(8).

Okolo, B. I., Adeyi, O., Oke, E. O., Agu, C. M., Nnaji, P. C., Akatobi, K. N., & Onukwuli, D. O. 2021. Coagulation kinetic study and optimization using response surface methodology for effective removal of turbidity from paint wastewater using natural coagulants. *Scientific African*, *14*, e00959.

Onu, C. E., Igbokwe, P. K., Nwabanne, J. T., & Ohale, P. E. 2022. ANFIS, ANN, and RSM modeling of moisture content reduction of cocoyam slices. *Journal of Food Processing and Preservation*, *46*(1), e16032.

Osman, A.I., El-Monaem, E.M.A., Elgarahy, A.M., Aniagor, C.O., Hosny, M., Farghali, M., Rashad, E., Ejimofor, M.I., López-Maldonado, E.A., Ihara, I. and Yap, P.S., 2023. Methods to prepare biosorbents and magnetic sorbents for water treatment: a review. *Environmental Chemistry Letters*, *21*(4), .2337-2398.

Tabrett, S., Ramsay, I., Paterson, B., & Burford, M. A. 2024. A review of the benefits and limitations of waste nutrient treatment in aquaculture pond facilities. *Reviews in Aquaculture*.

Usman, A. R., Kuzyakov, Y., Lorenz, K., & Stahr, K. 2006. Remediation of a soil contaminated with heavy metals by immobilizing compounds. *Journal of Plant Nutrition and Soil Science*, *169*(2), 205-212.

Van Staden, S. J., & Haarhoff, J. 2011. The use of filter media to determine filter cleanliness. *Physics and Chemistry of the Earth, Parts A/B/C*, *36*(14-15), 1135-1140.